Facial Selectivity in Epoxidation of 2-Cyclohexen-1-ol with Peroxy Acids. A Computational DFT Study

Mauro Freccero,[†] Remo Gandolfi,[†] Mirko Sarzi-Amadè,*[,†] and Augusto Rastelli[‡]

Dipartimento di Chimica Organica, Università di Pavia, V.le Taramelli 10, 27100 Pavia Italy, and Dipartimento di Chimica, Università di Modena, Via Campi 183, 41100 Modena, Italy

nmr@chifis.unipv.it

Received June 13, 2000

We addressed the mechanism of epoxidation of 2-cyclohexen-1-ol by locating all the transition structures (TSs) for the reaction of peroxyformic acid (PFA) with both pseudoequatorial and pseudoaxial cyclohexenol conformers (five TSs for each conformer) and, for purpose of comparison, also those for the PFA epoxidation of cyclohexene. Geometry optimizations were performed at the B3LYP/6-31G* level, energies refined with single point B3LYP/6-311+G**// B3LYP/6-31G* calculations and solvent effects introduced with the CPCM method. Our results can be summarized as follows: (i) all TSs exhibit a spiro-like structure, that is, the dihedral angle between the peroxy acid plane and the forming oxirane plane is closer to 90° than to 0° (or 180°); (ii) there is a stabilizing hydrogen bonding interaction in syn TSs that, however, is partly counteracted by unfavorable entropic effects; (iii) syn,exo TSs with hydrogen bonding at the PFA peroxy oxygens are definitely more stable than syn,endo TSs hydrogen bonded at the PFA carbonyl oxygen; (iv) facial selectivity of epoxidation of both cyclohexenol conformers is mostly the result of competition between only two TSs, namely, an anti,exo TS and its syn,exo counterpart. The latter TS is more stable than the former one, as stabilization by hydrogen bonding overrides the unfavorable entropic and solvent effects; (v) calculations correctly predict both the experimental dominance of attack leading to syn epoxide for both cyclohexenol conformers and the higher syn selectivity observed for the pseudoequatorial as compared to the pseudoaxial derivative. Moreover, also the experimental relative and absolute epoxidation rates for cyclohexene and cyclohexenol as well as for pseudoaxial and pseudoequatorial cyclohexenol derivatives are fairly well reproduced by computational data.

Introduction

Epoxidation with peroxy acids is one of the most important reaction for introduction of oxygen atoms into organic molecules.[1] Its widespread use in synthesis has certainly benefited from the Henbest's observation that the reaction of 2-cyclohexen-1-ol with peroxybenzoic acid is strongly facial selective with dominant (91%) attack by the peroxy acid on the same side of the OH group to produce the syn epoxide (Scheme 1).[2] Control of facial selectivity is obviously mandatory to fully exploit the synthetic potentialities of organic reactions. Thus, since Henbest's observation, several reports have further documented the ability of allylic hydrogen bond donor substituents (such as OH and NHCOR) to direct the stereochemical outcome of attacks by peroxy acids[3] and dioxiranes[4] to carbon−carbon double bonds.

On the mechanistic side the first spectacular breakthrough in the peroxy acid epoxidation field was provided, in the early 1950s,[5] by Bartlett's proposal of a transition structure featuring the concerted formation of the two new C- - -O bonds (**A** in Scheme 1). This model is now known as the "butterfly" TS and, even if stereochemical details have not been discussed by Bartlett, it looks like a "planar" TS, i.e., with the forming oxirane ring and the planar peroxy acid lying in the same plane. To explain the observed facial selectivity in the reaction of cyclic allylic alcohols, Henbest (1959) invoked a planar syn TS in which a hydrogen-bonding interaction involves the distal peroxy oxygen and the olefinic OH group in "outside" conformation (**B** in Scheme 1).[2a]

The possibility of a "spiro" TS for epoxidation of allylic alcohols (namely a TS in which the peroxy acid plane is perpendicularly oriented to the forming oxirane plane) was clearly raised but rejected by Whitham et al. (1970).[6] In fact, these authors argued that a spiro TS does not fulfill the geometrical requirements for an efficient hydrogen bonding involving the olefinic OH and the distal peroxy acid peroxy oxygen while a planar TS does.

A spiro-like (with an angle of ∼60° between the peroxy

* Corresponding author: Phone: +39 382 507668. Fax: +39 382 507323.

[†] Università di Pavia.

[‡] Università di Modena.

(1) Schwesinger, J. W.; Bauer, T. *Diastereoselective Epoxidation* in Stereoselective Synthesis; Helmchem, G.; Hoffmann, R. W.; Mulzer, J.; Schaumann, E., Eds.; Houben Weyl, Thieme: Stuttgart, New York, 1995; Vol. E21e, p 4599.

(2) (a) Henbest, H. B.; Wilson, R. A. L. *J. Chem. Soc.* **1959**, 1958. (b) For the reaction of 2-cyclohexen-1-ol with MCPBA in CH_2Cl_2 95% syn selectivity has been reported by Itoh, T.; Jitsukawa, K.; Kaneda, K.; Teranishi, S. *J. Am. Chem. Soc.* **1979**, *101*, 159.

(3) (a) Hoveyda, A. H.; Evans, D. A.; Fu, G. C. *Chem. Rev.* **1993**, *93*, 1307. (b) Kocovsky, P.; Stary, I. *J. Org. Chem.* **1990**, *55*, 3236. (c) Barili, P. L.; Berti, G.; Catelani, G.; D'Andrea, F.; DeRensis F. *Tetrahedron* **1997**, *53*, 8665.

(4) (a) Adam, W.; Mitchell, C. M.; Saha-Moller, C. H. *J. Org. Chem.* **1999**, *64*, 3699. (b) Yang, D.; Jiao, G. S.; Yip, Y. C.; Wong, M. K. *J. Org. Chem.* **1999**, *64*, 1635 (c) Murray, R. W.; Singh, M.; Williams, B. L.; Moncrieff, H. M. *J. Org. Chem.* **1996**, *61*, 1830. (d) Curci, R.; Dinoi, A.; Rubino, M. F. *Pure & Appl. Chem.* **1995**, *67*, 811.

(5) Bartlett, P. D. *Rec. Chem. Prog. 11*, **1950**, 47.

(6) Chamberlain P.; Roberts, M. L., Whitham, G. H. *J. Chem. Soc. (B)* **1970**, 1374.

10.1021/jo000900y CCC: $19.00
Published on Web 11/30/2000

Scheme 1

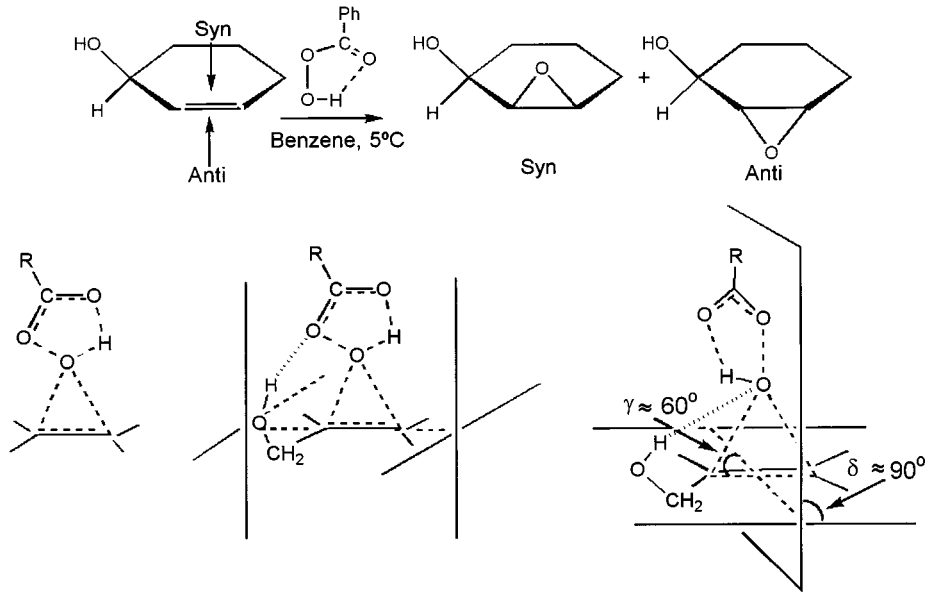

A: Bartlett's model (butterfly TS)

B: Henbest's model (planar TS)

C: Sharpless' model (spiro-like TS)

acid plane and the C=C bond axis) TS geometry but with hydrogen bonding to the proximal peroxy oxygen was proposed by Sharpless et al. (**C** in Scheme 1).[7]

Despite many other experimental investigations specifically aimed at producing experimental evidence useful for refining the proposed qualitative models, the TS geometry for the epoxidation of allylic alcohols remained ill defined and no general agreement was reached even on important details such as the planar-spiro dichotomy.[8,9]

The mechanism of olefin epoxidation, in particular that of allylic alcohols, by peroxy acid has represented a challenging task also for computational investigations. The presence of several heteroatoms with several lone pairs and the problem of the difficult to reproduce hydrogen bonding effects require high level calculations which must efficiently include electron correlation. Only recently DFT theory, in particular the B3LYP/6-31G* method, has enabled researchers to perform reliable calculations for epoxidations at a reasonable cost.[10]

Computational investigations, by Bach's[11a,b] and Houk's[11c,d] groups, of alkene epoxidations with peroxy acids definitely established the concerted formation of the two C- - -O bonds in a spiro or spiro-like TS exhibiting an almost collinear arrangement of the π orbital axis and the O- - -O breaking bond (i.e., an S_N2-like attack by the π bond on the peroxy system) and with charge transfer from olefin to peroxy acid.

As for allylic alcohols, after a pioneering study by Bach et al.,[12] a B3LYP/6-31G* investigation by our group disclosed the many facets of the peroxyformic acid (PFA) epoxidation of propenol.[13,14] For illustrative (of problems such as exo/endo, inside/outside, spiro/planar, basis set dependence of TS relative energies, etc.) purposes, the most stable five TSs, in which stabilizing hydrogen bonding is operative, are reported in Figure 1. It is worth stressing that hydrogen bonding influences the TS geometry, but it never causes the reacting system to abandon the spiro-like array of atoms in favor of a planar disposition. Calculations clearly revealed that hydrogen bonding can involve not only the peroxy oxygens (i.e., in syn,exo TSs, **F** and **G**), as assumed by experimentalists, but also the peroxy acid carbonyl oxygen (i.e., in syn,endo TSs, **D** and **E**) with the olefinic OH group occupying either an "inside" (**D** and **F**) or "outside" (**E** and **G**) conformational position. There is also an endo TS with hydrogen bonding at the peroxy oxygens, namely syn,endo′,out (**H**).

The relative potential energies of these five TSs are quite compressed, and, quite disappointingly, their order can be reversed by extending the basis set and on passing from potential energies to free enthalpies. For example, the syn,endo,in TS is calculated to be more stable than its syn,exo,in counterpart (Figure 1) by 1.8 kcal/mol with the B3LYP/6-31G* method and by 0.2 kcal/mol with the B3LYP/6-311+G** method, but it is predicted less stable by 0.61 kcal/mol when the B3LYP/6-311+G** free enthalpies are considered.[14]

(7) Sharpless, K. B.; Verhoeven, T. R. *Aldrichimica Acta* **1979**, *12*, 63.

(8) (a) Narula, A. S. *Tetrahedron Lett.* **1983**, *24*, 5421. (b) Rebeck, J., Jr.; Marshall, L.; McManis, J.; Wolac, R. *J. Org. Chem.* **1986**, *51*, 1649. (c) Kim, C.; Traylor, T. G.; Perrin, C. L. *J. Am. Chem. Soc.* **1998**, *120*, 9513. (d) Adam, W.; Degen, H. G.; Saha-Moller, C. H. *J. Org. Chem* **1999**, *64*, 1274. (e) Adam, W.; Mitchell, C. M.; Saha-Moller, C. H. *Eur. J. Org. Chem.* **1999**, *785*.

(9) Adam, W.; Wirth, T. *Acc. Chem. Res.* **1999**, *32*, 703.

(10) (a) Sim, F.; St-Amant, A.; Papai, I.; Salahub, D. R. *J. Am. Chem. Soc.* **1992**, *114*, 4391. (b) Novoa, J. J.; Sosa, C. *J. Phys. Chem.* **1995**, *99*, 15837.

(11) (a) Bach, R. D.; Glukhovtsev, M. N.; Gonzales, C.; Marquez, M.; Estevez, C. M.; Baboul, A. G.; Schlegel, H. B. *J. Phys. Chem. A* **1997**, *101*, 6092. (b) Bach, R. D.; Glukhovtsev, M. N.; Gonzales, C. *J. Am. Chem. Soc.* **1998**, *120*, 9902. (c) Singleton, D. A.; Merrigan, S. R.; Jian Liu; Houk, K. N. *J. Am. Chem. Soc.* **1997**, *119*, 3385. (d) Houk, K. N.; Liu, J.; DeMello, N. C.; Condroski, K. R. *J. Am. Chem. Soc.* **1997**, *119*, 10147.

(12) Bach, R. D.; Estévez, C. M.; Winter J. E.; Glukhovtsev, M. N. *J. Am. Chem. Soc.* **1998**, *120*, 680.

(13) Freccero, M.; Gandolfi, R.; Sarzi-Amadè M.; Rastelli, A. *J. Org. Chem.* **1999**, *64*, 3853.

(14) Freccero, M.; Gandolfi, R.; Sarzi-Amadè M.; Rastelli, A. *J. Org. Chem.* **2000**, *65*, 2030.

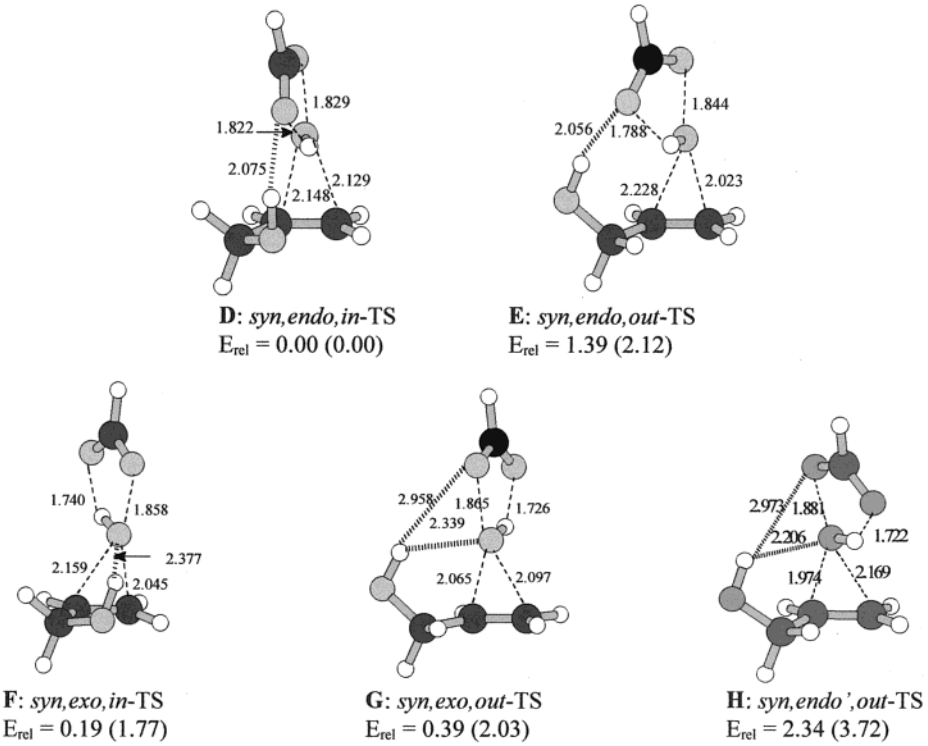

Figure 1. Optimized (B3LYP/6-311+G**) transition structures (bond lengths in Å) and their relative energies (E_{rel} in kcal/mol, B3LYP/6-31G* data in parentheses) for epoxidation of 2-propen-1-ol with peroxyformic acid.

This observation does not allow a fully unambiguous and definitive conclusion as to which kind of TSs endo (with H-bonding to carbonyl oxygen) or exo (with H-bonding to peroxy oxygens) should be dominant in the reaction of PFA with propenol and, in general, with acyclic alcohols.

We have already extended our theoretical study to the PFA epoxidation of chiral acyclic allylic alcohols fully confirming the mechanism found for propenol.[14] Moreover, despite the presence of several competing TSs with similar energies, B3LYP/6-311+G**//B3LYP/6-31G* calculations succeeded in reproducing fairly well the experimental facial selectivity of these substrates. However, the presence of many competing TSs made it impossible to choose two TSs, one for each of the two diastereotopic faces, as a basis for simple qualitative TS models useful to discuss facial selectivity of epoxidation of acyclic and, hopefully, cyclic allylic alcohols.

No theoretical studies have been produced to date for the reaction of cyclic allylic alcohols and, given the synthetic importance of epoxidation of these substrates, we feel that it is useful to fill this gap.

In fact, there should be similarities but also remarkable differences between the mechanism of epoxidation of cyclic allylic alcohols vs that of acyclic derivatives. Obviously, in the case of cyclic derivatives the olefinic OH group cannot adopt an "inside" conformation, but it is forced to assume an "outside" position. One can also anticipate that the relative role of endo (the olefinic OH group hydrogen bonds the peroxy acid carbonyl oxygen) and exo (the olefinic OH group hydrogen bonds the peroxy acid peroxy oxygens) TSs may change on passing from acyclic to cyclic derivatives.

We computationally addressed reactivity and facial selectivity of the most representative derivative in this class of compounds, i.e., 2-cyclohexen-1-ol, the actual substrate used in pioneering studies by Henbest. For purpose of comparison we have also investigated the cyclohexene epoxidation that provides the ideal model free from inductive and hydrogen bonding effects.

We aimed not only to reproduce the experimental data (reported in the following Section), to precisely define TS geometries (spiro/planar, exo/endo, outside/inside), to establish the mechanism and role of hydrogen bonding interaction but also to provide experimentalists with simple but reliable TS models useful for qualitative predictions and discussions about facial selectivity in cyclic allylic alcohol epoxidations.

Experimental Data for 2-Cyclohexenol Epoxidation with Peroxy Acids. Table 1 gathers the experimental data[2,3a,6] that are of relevance for this paper and, in particular, column 2 documents the dominance of syn attack driven by the allylic OH substituent. The experimental facial selectivity as well as the reaction rate of 2-cyclohexen-1-ol (**1**) epoxidation is certainly the composite result of the reactions of both pseudoequatorial (*eq*-**1**) and pseudoaxial (*ax*-**1**) conformers. In **1** the OH group seems to prefer the pseudoaxial position over the pseudoequatorial one by 0.97 kcal/mol.[15] At the reaction temperature the two conformers equilibrate rapidly with each other, and the conversion rate is certainly much faster (the inversion barrier for cyclohexene is ~5−6 kcal/mol) than the epoxidation rate. Thus, we are dealing with a Curtin−Hammett system for which product ratios only depend on the relative free enthalpies of the competing transition states.[16]

An approximate experimental evaluation of the facial selectivity (as well as of the reaction rate constant) of pseudoequatorial and pseudoaxial cyclohexenol conform-

(15) Senda, Y.; Imaizumi, S. *Tetrahedron Lett.* **1974**, *30*, 3813.
(16) Seeman, J. *Chem. Rev.* **1983**, *83*, 83.

Table 1. Syn/Anti Diastereoselectivity [Syn(%)/Anti(%)],[a] Relative (anti−syn) Free Enthalpy ($\Delta\Delta G^{\ddagger}_{anti-syn} = \Delta G^{\ddagger}_{anti} - \Delta G^{\ddagger}_{syn}$),[a] Rate Constant ($k \times 10^3$),[a,b] and Related Experimental Activation Parameters [$\Delta H^{\ddagger}$ and $\Delta G^{\ddagger}$ (kcal/mol), $\Delta S^{\ddagger}$ (eu)][b,c] for the Peroxybenzoic Acid Epoxidation of Cyclohexene, 2-Cyclohexen-1-ol, and Derivatives[a]

substrate	syn/anti %	$\Delta\Delta G^{\ddagger}$ anti−syn	$k \times 10^3$ (M^{-1} s^{-1})	$\Delta G^{\ddagger c}$	$\Delta H^{\ddagger b}$	$\Delta S^{\ddagger b}$
cyclohexene			6.33	18.95	10.42	−32.9
2-cyclohexen-1-ol	91:9	1.28	3.4	19.29	8.35	−41.0
2-cyclohexen-1-yl methyl ether	20:80	−0.77	0.42	20.44	12.36	−30.7
cis-5-*tert*-butyl-2-cyclohexen-1-ol	96:4	1.75	4.8	19.15		
trans-5-*tert*-butyl-2-cyclohexen-1-ol	84:16	0.91	0.67	20.24		

[a] In benzene at 278 K (ref 6). [b] Reference 3a. [c] Evaluated from the corresponding reaction rate constant.

Table 2. Relative Electronic Energies (E_{rel}), Dipole Moment (μ), and Some Representative Geometrical Parameters [Bond Lengths (Å) and Angles (deg)] for 2-Cyclohexen-1-ol Conformers (*eq*-1 and *ax*-1), *cis*- and *trans*-5-*tert*-butyl-2-cyclohexen-1-ol (*eq*-2 and *ax*-2), and Cyclohexene (3)

	E_{rel} (kcal/mol)	μ (Debye)	C=C	HOC_1C_2	$OC_1C_2C_3$	$C_2C_1C_6H_{ax}$	$C_3C_4C_5H_{ax}$	$C_1C_6C_5C_4$
eq-**1**	0.00	1.91	1.34	58.5	−140.7	−74.4	−77.6	−61.0
ax-**1**	0.05	1.95	1.34	−48.5	111.6	−77.2	−75.0	−60.2
eq-**2**	0.00	1.93	1.34	57.9	−140.1	−72.3	−71.4	−62.7
ax-**2**	0.10	1.94	1.34	−48.1	111.4	−75.3	−69.5	−61.4
3		0.23	1.34			−76.1[a]		−60.4[b]

[a] $C_1C_6C_5H_{ax}$. [b] $C_6C_5C_4C_3$

ers is provided by the epoxidations of the conformationally locked *cis*-(*eq*-**2**) and *trans*-5-*tert*-butyl-2-cyclohexen-1-ol (*ax*-**2**), respectively. It will be interesting to assess to what extent computational data can reproduce the higher facial selectivity and the higher reaction rate of the pseudoequatorial *eq*-**2** with respect to its pseudoaxial counterpart, *ax*-**2**.

A further interesting point is the slightly higher rate constant of cyclohexene than cyclohexenol epoxidation despite the stabilizing hydrogen-bonding interaction operative in the latter reaction. Experimental thermodynamic activation parameters[3a] suggest that cyclohexenol epoxidation [$\Delta H^{\ddagger} = 8.35$ kcal/mol, $\Delta S^{\ddagger} = -41.0$ eu, $\Delta G^{\ddagger} = 19.29$ kcal/mol] is favored by enthalpic factors while cyclohexene, slightly more, by entropic effects [$\Delta H^{\ddagger} = 10.42$ kcal/mol, $\Delta S^{\ddagger} = -32.9$ e.u., $\Delta G^{\ddagger} = 18.95$ kcal/mol]. The data for 3-methoxycyclohexene [$\Delta H^{\ddagger} = 12.36$ kcal/mol, $\Delta S^{\ddagger} = -30.7$ eu, $\Delta G^{\ddagger} = 20.44$ kcal/mol] clearly testify to a strong enthalpic rate retarding effect of an allylic OR group as a consequence of its inductive electron-attracting power. In the case of cyclohexenol epoxidation this effect is overcompensated by a stabilizing hydrogen bonding interaction which, however, can be held responsible for the highly negative activation entropy evaluated for this reaction (Table 1).

All these aspects deserve investigation by calculations in order to fully understand the mechanism of cyclic allylic alcohols epoxidation.

Computational Methods

Reactant as well as transition structure (TS) geometries for the reaction of peroxy formic acid (PFA) with 2-cyclohexen-1-ol (**1**) were fully optimized at the B3LYP/6-31G* theory level.[17] Since the relative energies for epoxidation TSs are basis set dependent,[18] it was mandatory to refine these energies with a larger basis set. Thus, for all TSs we performed single point calculations with the B3LYP/6-311+G** method on B3LYP/6-31G* geometries. The reliability of the latter calculation protocol is supported by previous observations:[13,14] (i) B3LYP geometries of epoxidation TSs are largely independent of the basis set used, e.g., on passing from 6-31G* to 6-311+G**, (ii) B3LYP/6-311+G**//B3LYP/6-31G* relative and absolute TS energies are nearly the same as those obtained by full B3LYP/6-311+G** optimization, (iii) the trend of relative energies obtained by the B3LYP/6-311+G** method is similar to that given by the very reliable (but much more expensive) B3LYP/AUG-cc-pVTZ method, (iv) B3LYP calculations with basis set of 6-311+G** or similar quality have been largely used to investigate hydrogen bonding interactions with good results.[10b,19] Points i and ii have been positively checked also in this work for four (Table 6) out the ten TSs by carrying out full geometry optimization with the 6-311+G** basis set.

Full geometry optimization of the stationary structures were performed by utilizing gradient geometry optimization and default threshold for convergence as implemented in the Gaussian 98 suite of programs.[20] All critical points have been characterized by diagonalizing the Hessian matrixes calculated for the optimized structures. Relative energies and representative geometrical data for cyclohexene (**3**) and for the two conformers with the OH group in pseudoequatorial (*eq*-**1** and *eq*-**2**) and, respectively, pseudoaxial (*ax*-**1** and *ax*-**2**) position of cyclohexenol as well as of *cis*- and *trans*-5-*tert*-butyl-2-cyclohexen-1-ol are reported in Table 2 while graphical presentations are reported in Figure 3.

Transition structures have only one negative eigenvalue (first-order saddle points) with the corresponding eigenvector involving the expected formation of the two new oxirane bonds, the cleavage of the O_7-O_8, the

(17) (a) Becke, A. D. *J. Chem. Phys.* **1993**, *98*, 1372. (b) Lee, C.; Yang, W.; Parr, R. G. *Phys. Rev. B* **1988**, *37*, 785.

(18) It is important to recall that the most important effect of basis set extension and introduction of diffuse functions is that of decreasing the energy of syn,exo (by ∼ 1.5 kcal/mol) and anti (by ∼ 2.5 kcal/mol) TSs with respect to that of syn,endo TSs.

(19) (a) Salvatella, L.; Ruiz-Lopez, M. F. *J. Am. Chem. Soc.* **1999**, *121*, 10772. (b) McDermott, A. E.; Wei, Y.; de Dios, A. C. *J. Am. Chem. Soc.* **1999**, *121*, 10389.

(20) Gaussian 98, Revision A.6, M. J. Frisch, G. W. Trucks, H. B. Schlegel, G. E. Scuseria, M. A. Robb, J. R. Cheeseman, V. G. Zakrzewski, J. A. Montgomery, Jr., R. E. Stratmann, J. C. Burant, S. Dapprich, J. M. Millam, A. D. Daniels, K. N. Kudin, M. C. Strain, O. Farkas, J. Tomasi, V. Barone, M. Cossi, R. Cammi, B. Mennucci, C. Pomelli, C. Adamo, S. Clifford, J. Ochterski, G. A. Petersson, P. Y. Ayala, Q. Cui, K. Morokuma, D. K. Malick, A. D. Rabuck, K. Raghavachari, J. B. Foresman, J. Cioslowski, J. V. Ortiz, B. B. Stefanov, G. Liu, A. Liashenko, P. Piskorz, I. Komaromi, R. Gomperts, R. L. Martin, D. J. Fox, T. Keith, M. A. Al-Laham, C. Y. Peng, A. Nanayakkara, C. Gonzalez, M. Challacombe, P. M. W. Gill, B. Johnson, W. Chen, M. W. Wong, J. L. Andres, C. Gonzalez, M. Head-Gordon, E. S. Replogle, and J. A. Pople, Gaussian, Inc., Pittsburgh, PA, 1998.

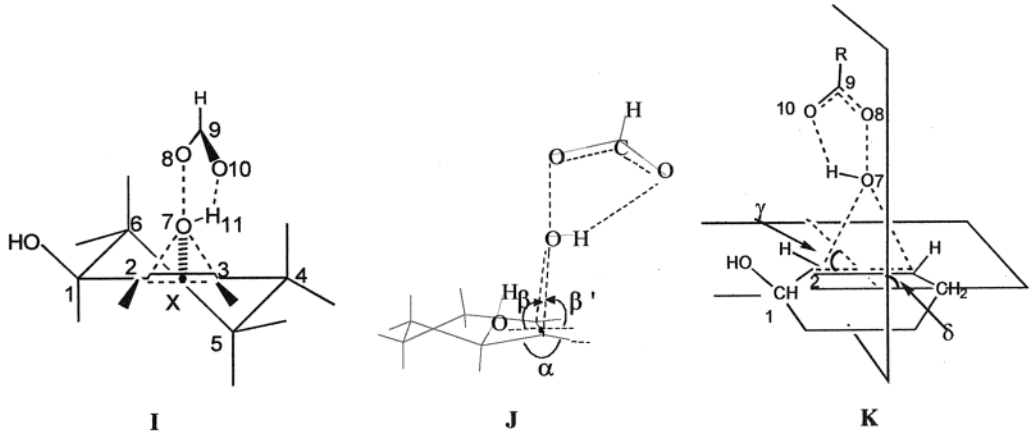

Figure 2. Schematic representation of *syn,exo,eq*-**5** TS of peroxyformic acid epoxidation of cyclohexenol.

lengthening of the $C_9{=}O_{10}$, and the shortening of the $O_8{-}C_9$ peroxy acid bonds (see **I** in Figure 2 for TS numbering). The imaginary frequencies (cm^{-1}) of the TSs are reported (as ν_i) in Table 3 for cyclohexene TSs and in Table 4 for the cyclohexenol TSs. The search for TSs was limited to concerted transition structures, i.e., only restricted B3LYP methods have been used. However, the wave function stability for all first-order saddle points was checked positively.

The B3LYP/6-31G* TS geometries for the cyclohexene and cyclohexenol epoxidation are reported in Figure 4 and Figure 5 with some relevant bond lengths. In addition to α, β, and β' angles (see **J**, Figure 2), the following angles are reported in Table 3 and Table 4 for the cyclohexene and cyclohexenol reaction, respectively: (i) the $H{-}O{-}C_1{-}C_2$ (to describe rotation around the $O{-}C_1$) and $O{-}C_1{-}C_2{-}C_3$ torsional angles; (ii) the $X{-}O_7{-}O_8$ angle which allows one to evaluate the alignment of the axis of the π cloud with the breaking O_7- - -O_8 bond (X is a dummy atom placed at the center of the C═C bond, see **I** in Figure 2); a value lower than 180° indicate that O_8 is bent toward the side of the C═O- - -H peroxy acid moiety; (iii) the $H_{11}{-}O_7{-}O_8{-}C_9$ and $O_7{-}O_8{-}C_9{-}O_{10}$ torsional angles related to out-of-plane distortion of the peroxy acid moiety; (iv) $|180° - \alpha|$ (with α being the dihedral angle between the mean planes $H{-}C_2{-}C_3{-}H$ and $C_1{-}C_2{-}C_3{-}C_4$) which describes out-of-plane distortion of the olefinic moiety (see **J** in Figure 2); (v) β and β' (**J** in Figure 2), that is, the dihedral angles between the forming oxirane plane and the $C_1{-}C_2{-}C_3{-}C_4$ and $H{-}C_2{-}C_3{-}H$ mean planes, respectively; (vi) $H_{11}{-}O_7$-X$-C_2$ [$H_{11}{-}O_7$-X$-C_1$ for cyclohexene] angle describes the H_{11} hydrogen peroxy acid rotation away from the perfect spiro conformation; (vii) γ, the angle between the $O_7{-}O_8{-}C_9$ plane of the attacking peroxy acid and the C═C bond axis. A value lower than 90° means that the C_9O_{10} peroxy acid fragment is closer to C_2 [C_1 for cyclohexene] than to C_3 [C_2 for cyclohexene] (see **K**, Figure 2) as a result of rotation around the O_7- - -O_8 bond; (viii) δ, the dihedral angle between the $O_7{-}O_8{-}C_9$ plane of the peroxy acid and the mean plane of the double bond moiety. A value larger (smaller) than 90° means that the peroxy acid plane is tilted away from (toward) the $C_1{-}OH$ [$C_6{-}H_{eq}$ for cyclohexene] group.

A value of 90° for H_{11}-O_7-X$-$C, γ and δ corresponds to a symmetrical "spiro" structure while a "planar" structure requires a value of 0° (or 180°) for both H_{11}-O_7-X$-$C and γ and of 90° for δ.

Cartesian coordinates of reactants and all TSs are available on request.

To produce theoretical activation parameters, vibrational frequencies in the harmonic approximation were calculated for all the optimized B3LYP/6-31G* structures and used, unscaled,[21] to compute the zero point energies, entropy, and thermal corrections to enthalpy. The B3LYP/6-31G* enthalpy, entropy, and free enthalpy are reported as Supplementary Information (Tables S1 and S2). Moreover, the B3LYP/6-31G* molecular motion contributions were used with the B3LYP/6-311+G**//B3LYP/6-31G* electronic energies to evaluate the gas-phase B3LYP/6-311+G**// B3LYP/6-31G* enthalpy, entropy, and free enthalpy (Tables 5 and 7).

The computed enthalpy, entropy, and free enthalpy were converted from the 1 atm standard state into the standard state of molar concentration (ideal mixture at 1 mol/L and 1 atm) in order to use them for a direct comparison with the experimental results in solution where the latter activity scale is generally used.[22,23]

The contribution of solvent effects to the activation free enthalpy of the reactions under study were calculated via the self-consistent reaction field (SCRF) method using the CPCM model (as implemented in Gaussian 98) which includes the nonelectrostatic terms (cavitation, dispersion, and repulsion energy) in addition to the classical electrostatic contribution.[24] Solvation effect has been evaluated for benzene solution by single point calculation (i.e., with unrelaxed gas-phase reactant and TS geometries) at the B3LYP/6-31G* level and used to evaluate both the B3LYP/6-31G* and B3LYP/6-311+G**//B3LYP/6-31G* solution free enthalpies.

(21) Rastelli, A.; Bagatti, M.; Gandolfi, R. *J. Am. Chem. Soc.* **1995**, *117*, 4965.

(22) For conversion from 1 atm standard state to 1 mol/L standard state, the following contributions need to be added to standard enthalpy, entropy, and free enthalpy: $-RT$, $-R - R \ln R'T$ and $RT \ln R'T$ where R' is the value of R in L × atm/mol × K.[23a] For a reaction with A + B = C stoichiometry, the corrections for $\Delta H^{\ddagger}$, $\Delta S^{\ddagger}$, and $\Delta G^{\ddagger}$ are RT, $RT + RT \ln R'T$, and $-RT \ln R'T$, respectively. Finally, at 278 K the corrections amount to 0.55 and −1.72 kcal/mol for $\Delta H^{\ddagger}$ and $\Delta G^{\ddagger}$, respectively, and 8.20 eu for $\Delta S^{\ddagger}$.[21,23b] To avoid misunderstanding, let us emphasize that the corrected theoretical data are still intended for gas-phase reactions.

(23) (a) Benson, S. Thermochemical Kinetics, Wiley: New York, 1968; p.8. (b) Jorgensen, W. L.; Lim, D.; Blake, J. F. *J. Am. Chem. Soc.* **1993**, *115*, 2936. (c) In particular it is not established whether the "free" volume available for the solute molecules corresponds to the whole volume of the solution or to a small part (e.g., 1%) of it. See refs 23b and 24d.

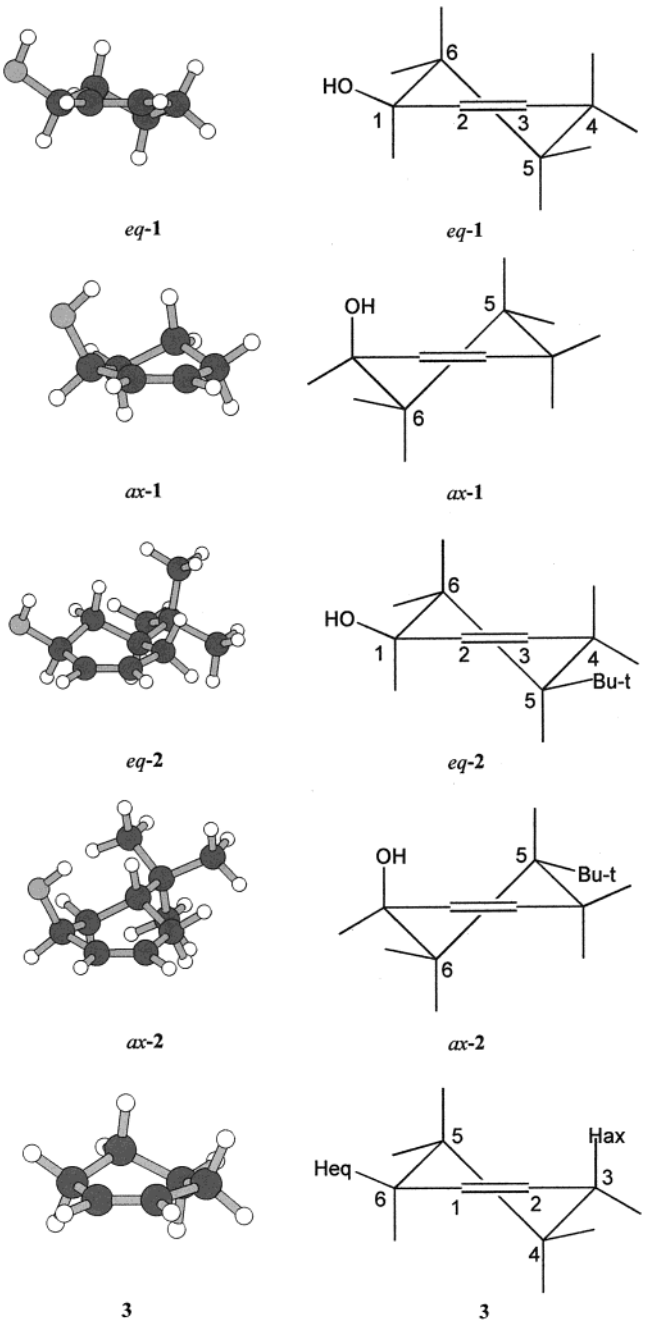

Figure 3. B3LYP conformational minima of pseudoequatorial (*eq*-**1**) and pseudoaxial (*ax*-**1**) 2-cyclohexen-1-ol, *cis*-(*eq*-**2**) and *trans*-5-*tert*-butyl-2-cyclohexen-1-ol (*ax*-**2**), and cyclohexene (**3**).

Cyclohexenol Conformers. Cyclohexenol consists of a fast equilibrating mixture of two ring conformers with the OH group in pseudoequatorial ($OC_1C_2C_3 \approx 140°$) and pseudoaxial ($OC_1C_2C_3 \approx 111°$) position. Moreover, rotation of the OH bond around the C_1-O bond gives rise to three rotamers for both the ring conformers. We located all these six minima, but only the lowest energy minimum, for both the pseudoequatorial (*eq*-**1**) and pseudoaxial (*ax*-**1**) conformer,[25] are reported in Figure 3 and Table 2. In both *eq*-**1** and *ax*-**1** the O−H bond points toward the double bond and is properly oriented to be involved in hydrogen bonding with the attacking peroxy acid. These two isomers exhibit the very same free enthalpy both in gas phase and in solution: thus, the theoretically predicted ~1/1 ratio does not satisfactorily reproduces the claimed experimental dominance of the pseudoaxial isomer (84%).[15]

The theoretical facial selectivity data obtained for cyclohexenol conformers (**1**) can be meaningfully compared to the experimental results obtained for the corresponding 5-*tert*-butyl-2-cyclohexen-1-ol (**2**) isomers only if the geometries of the *tert*-butyl-substituted and the corresponding unsubstituted conformer are similar. Actually, they are very similar to each other as shown, for example, by the ring puckering (see the $C_1C_6C_5C_4$ torsional angle in Table 2) and by the $OC_1C_2C_3$ and HOC_1C_2 torsional angles in **1** as compared to those in **2**. Similarity of the latter two angles in **1** and **2** clearly indicates that hydrogen bonding to the attacking peroxy acid can be as efficient in compounds **2** as it is in compounds **1**.

The only significant geometry difference between unsubstituted **1** and substituted **2** cyclohexenols is a slight decrease in the $C_3C_4C_5H_5$ and $C_2C_1C_6H_6$ torsional angles on passing from the former compounds to the latter ones. The presence of the bulky *tert*-butyl group in compounds **2** induces a small inside rotation of both axial H-5 (by 6°) and axial H-6 (by 2°) (Table 2).

Transition Structures for Cyclohexene Epoxidation: Steric and Torsional Effects. TSs for PFA epoxidation of cyclohexene are free from effects on geometry due to hydrogen bonding and inductive effects and should reflect only the intrinsic requirements of a cyclohexene skeleton. We located two TSs (Figure 4) corresponding to the exo (*exo*-**4**) and endo (*endo*-**4**, i.e., with the H- - -O=C moiety on the same side of the cyclohexene ring) approach of the peroxyformic acid (PFA).[26] As there is not a symmetry plane bisecting the double bond of the half-chair cyclohexene form, one should anticipate that cyclohexene epoxidation TSs cannot exhibit synchronous C- - -O bond formation while also the γ and $H_{11}-O_7-X-C_1$ angles must deviate somewhat from a perfect (90°) spiro geometry.

Actually, in *exo*-**4** a small rotation around the O_7- - -O_8 (by 4°, i.e., $\gamma = 94°$, Table 3) and tilting (by 2°, i.e., $\delta = 88°$) of the peroxy acid moiety is enough to accommodate steric crowding, due to the "up" methylene at position 5 and to the axial H at position 3 of the cyclohexene fragment while asynchronicity in bond formation is of 0.065 Å. In the case of endo approach deviation from a spiro orientation is more pronounced,

(24) (a) Cramer, C. J.; Truhlar, D. G. *Chem. Rev.* **1999**, *99*, 2161. (b) Barone, V.; Cossi, M. *J. Phys. Chem.* **1998**, *102*, 1995. (c) Tomasi, J.; Persico, M. *Chem. Rev.* **1994**, *94*, 2027. (d) Arnaud, R.; Adamo, C.; Cossi, M.; Milet, A.; Vallée; Y., Barone, V. *J. Am. Chem. Soc.* **2000**, *122*, 324.

(25) The other two rotamers (i.e., those ones with the OH hydrogen atom pointing away from the double bond) have a B3LYP/6-311+G**// B3LYP/6-31G* potential energy (free enthalpy) that is higher than either *eq*-**1** by 0.77 and 0.89 (0.60 and 0.60) kcal/mol or *ax*-**1** by 0.68 and 1.09 (0.29 and 0.99) kcal/mol. The higher stability of *eq*-**1** or *ax*-**1** with respect to their rotational counterparts can be attributed to both the weak OH- - -π stabilization in the former and to the repulsion between the electron cloud of the oxygen lone pairs and that of the double bond in the latter. The calculated equilibrium constant between pseudoaxial and pseudoequatorial cyclohexenol is close to 1/1 even if all the rotamers are taken into account.

(26) We managed to locate only one exo and one endo TS for cyclohexene epoxidation even if rotation around the O_7- - -O_8 bond can, in principle, produce other first-order saddle points. In fact, in the case of syn attack to both *eq*-**1** and *ax*-**1** we could locate two endo TSs, indicated as syn,endo and syn,endo′, while in the case of anti attack only one endo-type saddle point, that one which minimizes steric crowding, was located for both conformers.

Table 3. Bond lengths (Å), angles (deg), and dipole moment (μ, Debye) for the TSs of the PFA epoxidation of cyclohexene (3) at the B3LYP/6-31G* level[a]

parameter	C_1-C_2	O_8-O_9	C_9-O_{10}	$X-O_7-O_8$	$H_{11}-O_7-X-C_1$	γ	δ	μ
exo-**4**	1.374	1.291	1.235	178.6	91.5	93.6	88.1	0.31
endo-**4**	1.374	1.289	1.237	177.4	101.8	104.5	88.2	0.30

[a] For both TSs: the peroxy acid moiety is planar $H_{11}-O_7-O_8-C_9 \leq 1.6°$, imaginary frequency ≈ 405 cm^{-1}, electron transfer (from **3** to PFA) ≈ 0.30, CHeplG net atomic charges on: $O_7 = -0.3$; $O_8 = -0.4$; $O_{10} = -0.6$.

Table 4. Bond Lengths (Å), Angles (deg), Imaginary Frequency (ν_i), OH Stretching Frequency (ν_{OH}), Dipole Moment (μ), Electron Transfer (from 1 to PFA), and Net Atomic Charges for the TSs of the PFA Epoxidation of *eq*-1 and *ax*-1 at the B3LYP/6-31G* Level[a,b]

parameter	syn,exo *eq*-**5**	syn,endo *eq*-**5**	syn,endo′ *eq*-**5**	anti,exo *eq*-**5**	anti,endo *eq*-**5**	syn,exo *ax*-**5**	syn,endo *ax*-**5**	syn,endo′ *ax*-**5**	anti,exo *ax*-**5**	anti,endo *ax*-**5**
C_2-C_3	1.372	1.374	1.376	1.374	1.376	1.376	1.374	1.378	1.376	1.376
O_8-C_9	1.293	1.284	1.290	1.290	1.287	1.291	1.286	1.286	1.290	1.288
C_9-O_{10}	1.234	1.242	1.236	1.236	1.239	1.236	1.241	1.238	1.237	1.239
$H-O-C_1-C_2$	54.1	69.7	47.9	69.2	68.1	−38.9	−60.3	−25.5	−64.0	−64.6
$O-C_1-C_2-C_3$	−142.1	−141.4	−146.7	−141.2	−142.2	113.1	120.4	122.7	107.1	107.6
$X-O_7-O_8$	177.7	174.6	174.2	178.1	176.8	178.9	174.3	175.9	178.7	176.9
$H_{11}-O_7-X-C_2$	95.3	71.4	128.3	86.7	79.0	82.7	72.9	132.6	92.6	105.3
$O_7-O_8-C_9-O_{10}$	0.11	4.1	0.8	0.0	0.7	0.4	2.2	1.51	0.3	0.6
$H_{11}-O_7-O_8-C_9$	0.11	17.5	0.3	0.8	1.2	1.2	9.1	1.51	0.4	1.2
$\lvert 180° - \alpha \rvert$	5.29	5.8	6.7	6.9	7.4	4.6	5.8	7.07	7.5	8.1
β	92.8	103.3	100.0	94.2	102.7	92.1	102.6	100.3	94.3	102.8
β'	92.4	82.5	86.6	92.7	84.7	92.4	83.1	86.7	93.2	85.4
γ	102.4	54.0	132.5	85.1	76.1	83.6	63.4	133.6	96.8	108.7
δ	80.0	80.4	80.3	93.7	86.7	91.1	89.3	85.5	85.5	86.6
ν_i (cm^{-1})	392	393	395	418	422	390	411	384	417	423
ν_{OH} (cm^{-1})	3689	3616	3686	3721	3719	3680	3636	3675	3730	3728
μ (Debye)	3.73	3.83	3.87	4.61	5.88	3.89	3.66	4.35	4.04	3.98
electron tranfer	0.30	0.30	0.32	0.30	0.32	0.28	0.27	0.33	0.29	0.32
net charge on O_7[c]	−0.31	−0.29	−0.31	−0.29	−0.29	−0.28	−0.29	−0.31	−0.32	−0.28
O_8	−0.41	−0.40	−0.39	−0.40	−0.41	−0.40	−0.38	−0.41	−0.40	−0.40
O_{10}	−0.57	−0.60	−0.55	−0.56	−0.57	−0.55	−0.57	−0.56	−0.56	−0.51

[a] O_7-H_{11} bond length in TSs **5** spans the range = 0.983−1.003 Å. [b] HCOOOH ground-state geometry: O_7-O_8: 1.441 Å; O_8-C_9:1.341 Å; C_9-O_{10}: 1.201 Å; O_7-H_{11}: 0.981 Å, H−O−O−C and O−O−C−O = 0°; μ = 1.35 D; CHelpG net atomic charges: $O_7 = -0.34$; $O_8 = -0.21$; $O_{10} = -0.49$. [c] Net atomic charge on O_7H group is always ≈ 0.08.

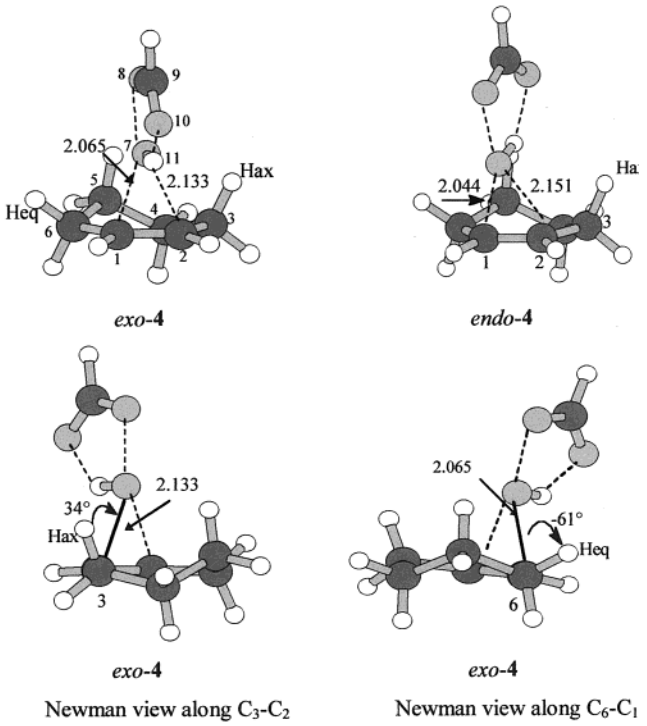

Figure 4. B3LYP optimized transition structures (bond lengths in Å) for epoxidation of cyclohexene with peroxyformic acid.

namely γ increases to 104° in *endo*-**4**, while asynchronicity in bond formation rises to 0.11 Å with the longer bond next to C−H at position 3.

One can emphasize that the observed asynchronicity tends to promote a reduction in the eclipsing between the longer C_2- - -O_7 forming bond and the allylic axial C_3-H. Figure 4 illustrates (for *exo*-**4**) the observation that the torsional interaction between the C_2- - -O_7 forming bond and the axial C_3-H is definitely stronger (torsion angle $\approx$ 34°) than that between the C_1- - -O_7 incipient bond and the equatorial C_6-H (torsion angle $\approx$ 61°). One can easily deduce that the former interaction would have been even slightly worse if O_7 was symmetrically placed above the C_1-C_2 bond. Thus, the different conformation of the two allylic C−H bonds (syn with respect to the attacking peroxy acid) flanking the C=C bond can be held responsible, at least in part, for the observed asynchronicity in bond formation.[27,28]

Geometry of Transition Structures for 2-Cyclohexen-1-ol Epoxidation. In the case of cyclohexenol we located, by the B3LYP/6-31G* method, ten TSs, that is, three syn and two anti TSs for both *eq*-**1** and *ax*-**1**. Both syn and anti, with respect to the OH group, attacks can take place with either an endo or exo orientation. All TSs are reported in Figure 5 and are given descriptors that indicate all their relevant features. For example, *syn,-exo,eq*-**5** indicates a TS deriving from an exo (i.e., with

(27) The importance of torsional strain as important stereoselective controlling effect in epoxidation reactions has already been advanced by Houk et al.: (a) Lucero, M. J.; Houk, K. N. *J. Org. Chem.* **1998**, *63*, 6973. (b) Martinelli, M. J.; Peterson, B. C.; Khau, V. V.; Hutchinson, D. R.; Leanna, M. R.; Audia, J. E.; Droste, J. J.; Wu, Y. D.; Houk, K. N. *J. Org. Chem.* **1994**, *59*, 2204.

(28) Vedejs, E.; Dent, W. H., III; Kendall, J. T.; Oliver, P. A. *J. Am. Chem. Soc.* **1996**, *118*, 3556.

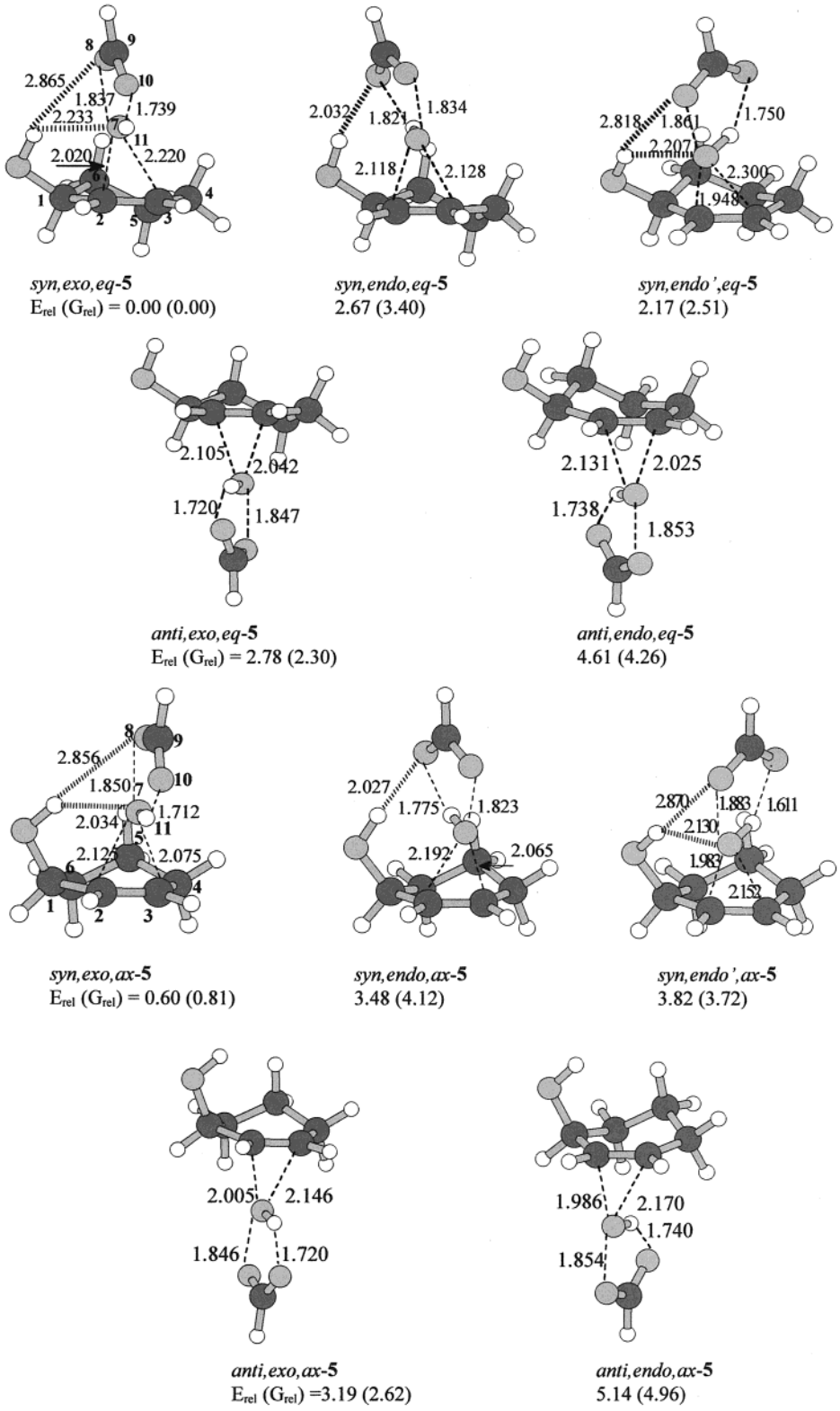

Figure 5. B3LYP optimized transition structures (bond lengths in Å) for epoxidation of 2-cyclohexen-1-ol with peroxyformic acid. Relative (kcal/mol) electronic energy and free enthalpy (data in parentheses) at the B3LYP/6-311+G**//B3LYP/6-31G* level.

the C═O- -H peroxy acid moiety pointing away from the ring) attack by PFA on the syn face of conformer *eq*-**1**.

Four TSs were also optimized at the B3LYP/6-311+G** level, and their geometries (Table 6) are quite similar to those obtained by the lower method (Table 4), thus confirming that B3LYP/6-31G* calculations are adequate to reliably describe the geometrical structure of these TSs.

Hydrogen Bonding Effect on Geometries. In all the syn TSs located by us the olefinic OH group is involved as a donor in a hydrogen bonding interaction with PFA acting as acceptor either at the peroxy oxygens or at the carbonyl oxygen. In syn,exo TSs (*syn,exo,eq*-**5** and *syn,exo,ax*-**5**, Figure 5) the PFA peroxy oxygen atoms accept the hydrogen bond while in syn,endo TSs (*syn,endo,eq*-**5** and syn,*endo,ax*-**5**) the more basic carbonyl

Table 5. Electronic Energies (hartree), Relative Electronic Energies ($E^{\ddagger}_{rel}$, kcal/mol), Electronic Activation Energies ($\Delta E^{\ddagger}$), Activation Parameters [$\Delta H^{\ddagger}$, $\Delta S^{\ddagger}$, $\Delta G^{\ddagger}$ (gas phase), and $\Delta G^{\ddagger}_{sol}$ (solution)], Relative Free Enthalpies [$G^{\ddagger}_{rel}$ (gas phase) and $G^{\ddagger}_{sol,rel}$ (solution)] for PFA Epoxidation of 2-Cyclohexen-1-ol at the B3LYP/6-311+G//B3LYP/6-31G* Level**

TS	energies[a]	$E^{\ddagger}_{rel}$		$\Delta E^{\ddagger}$	$\Delta H^{\ddagger b}$	$\Delta S^{\ddagger b}$	$G^{\ddagger}_{rel}$[b]		$\Delta G^{\ddagger b}$	$\delta G^{\ddagger}_{sol}$[c]	$G^{\ddagger}_{sol,rel}$[c]		$\delta\Delta G^{\ddagger}_{sol}$	$\Delta G^{\ddagger}_{sol}$[d]
eq-**1**	−309.955519	0.00					0.02			−1.86	0.00			
ax-**1**	−309.955463	0.03					0.00			−1.81	0.03			
PFA	−264.972745									−0.87				
syn,exo,eq-**5**	−574.914175	0.00		8.84	9.33	−31.33	0.00		18.05	−1.70	0.00		1.03	19.08
syn,endo,eq-**5**	−574.909922	2.67		11.51	12.13	−33.28	3.40		21.45	−1.28	3.82		1.45	22.90
syn,endo′,eq-**5**	−574.910717	2.17		11.01	11.52	−32.47	2.51		20.56	−1.29	2.92		1.44	22.00
anti,exo,eq-**5**	−574.909738	2.78		11.62	12.01	−29.96	2.30		20.35	−2.71	1.29		0.02	20.37
anti,endo,eq-**5**	−574.906831	4.61		13.45	13.89	−30.26	4.26		22.31	−2.36	3.60		0.37	22.68
syn,exo,ax-**5**	−574.913222	0.60	0.00	9.40	9.94	−32.05	0.81	0.00	18.87	−1.59	0.92	0.00	1.09	19.96
syn,endo,ax-**5**	−574.908639	3.48	2.88	12.28	12.93	−33.17	4.12	3.31	22.18	−1.04	4.78	3.86	1.64	23.82
syn,endo′,ax-**5**	−574.908095	3.82	3.22	12.62	12.92	−31.77	3.72	2.91	21.78	−1.47	3.95	3.03	1.21	22.99
anti,exo,ax-**5**	−574.909087	3.19	2.59	11.99	12.35	−29.88	2.62	1.81	20.68	−2.53	1.79	0.87	0.15	20.83
anti,endo,ax-**5**	−574.905982	5.14	4.54	13.94	14.46	−30.69	4.96	4.15	23.02	−2.06	4.60	3.68	0.62	23.64

[a] Energies from B3LYP/6-311+G** single point calculations on fully optimized B3LYP/6-31G* geometries. [b] For evaluation of the thermodynamic properties, the B3LYP/6-31G* computed kinetic contributions are used; rigid rotor-harmonic oscillator approximation assumed; energies in kcal/mol, entropy in cal/mol K; standard state (278.15 K) of the molar concentration scale (gas in ideal mixture at 1 mol/L, P = 1 atm); $\Delta H^{\ddagger}$, $\Delta G^{\ddagger}$ are the molar activation enthalpy and free enthalpy; $\Delta S^{\ddagger}$ is the molar activation entropy. For conversion from 1 atm standard state to 1 mol/L standard state (both for gas phase), see ref 21. [c] Solvent (benzene) effect (kcal/mol) is introduced by using the CPCM model at the B3LYP/6-31G* level: $\delta\ G^{\ddagger}_{sol} = G^{\ddagger}_{sol} - G^{\ddagger}_{gas}$. [d] $\Delta G^{\ddagger}_{sol}$ includes the $\delta\ \Delta G^{\ddagger}_{sol}$ correction ($\Delta G^{\ddagger}_{sol} = \Delta G^{\ddagger} + \delta\ \Delta G^{\ddagger}_{sol}$).

Table 6. Relative Electronic Energies (E_{rel}, kcal/mol)[a] and Some Geometrical Parameters (bond lengths in angstroms and angles in degrees) for the Four Most Representative TSs Evaluated at the B3LYP/6-311+G Level**

TS	E_{rel}	C_2-C_3	C_2-O_7	C_3-O_7	O_7-O_8	$O-C_1-C_2-C_3$
syn,exo,eq-**5**	0.00	1.370	2.053	2.241	1.845	−143.4
syn,endo,eq-**5**	2.63	1.370	2.182	2.121	1.851	−141.9
anti,exo,eq-**5**	2.84	1.371	2.122	2.083	1.858	−141.1
syn,exo,ax-**5**	0.65	1.372	2.113	2.142	1.856	115.1

[a] Electronic energy for *syn,exo,eq*-**5** = 574.913639 hartree.

oxygen[12] plays that role. However, syn,endo TSs ($\gamma \approx 58°$) are sterically crowded and steric congestion can partially be relieved by rotation around the O_7- - -O_8 bond to give further endo TSs, i.e., syn,endo′ TSs, in which the peroxy oxygens have replaced the carbonyl oxygen as hydrogen bond acceptor. In the latter TSs the γ angle ($\approx$130°) highly deviates from 90° in order to maximize hydrogen bonding.

All the TSs exhibit several geometry features (Table 4) already present in TSs for the reaction of PFA with acyclic allylic alcohols. In short, (i) out of plane distortion of the alkene fragment (α) and elongation of the C=C and C_9-O_{10} bonds as well as shortening of the C_9-O_8 bond are small, indicating early TSs, (ii) the forming oxirane ring is almost symmetrically disposed with respect to the two sides of the C=C bond with $\beta \sim \beta'$; only in endo type TSs is β slightly larger than β', (iii) there is a surprisingly strict alignment of the π bond axis with the breaking O_7- - -O_8 bond (i.e., $XO_7O_8 \sim 174°-180°$) in accord with the S_N2-like character of these reactions, (iv) electron transfer from olefin to peroxy acid is of $\approx$ 0.3 electrons. The largest negative charge (Table 4) is located on the carbonyl oxygen (≈ -0.60) while that on the distal oxygen ($O_8 \approx -0.40$) is larger than that on the proximal one ($O_7 \approx -0.30$, O_7H_{11} as a whole $\approx$ 0.08).

A central point in the peroxy acid epoxidation mechanism is represented by competition between TSs with hydrogen bonding to peroxy oxygens and those with hydrogen bonding to carbonyl oxygen. The latter TSs must have an endo stucture (*syn,endo,eq*-**5** and *syn,endo,ax*-**5**) while in the former the peroxy acid can adopt, as underlined above, either an exo (*syn,exo,eq*-**5** and *syn,exo,ax*-**5**) or an endo orientation (*syn,endo′,eq*-**5** and *syn,endo′,ax*-**5**). Hydrogen bonding to the carbonyl oxygen is stronger than hydrogen bonding to the peroxy oxygens as testified by the lower (by $\sim$50−70 cm^{-1}) OH stretching frequency in TSs that take advantage of the former interaction than in those that benefit from the latter one.

However, formation of the strong intermolecular hydrogen bond involving the carbonyl oxygen, as in syn,endo TSs, inevitably brings about a weakening of the intramolecular peroxy acid hydrogen bond as clearly shown by a larger O_{10}- - -H_{11} distance, in comparison to that of related syn,exo TSs, and by the substantial out of plane distortion of H_{11}. *In fact, while in all TSs with hydrogen bonding to the peroxy oxygens (syn,exo and syn,endo′) the peroxy acid moiety maintains its ground state planar array of atoms, in syn,endo,eq*-**5** *and syn,endo,ax*-**5** *H-11 is pushed out of the heavy atom peroxy acid plane (H_{11}-O_7-O_8-C_9 = 17° and 9°, respectively)*. Thus, geometry data demonstrate that the more favorable intermolecular hydrogen bonding interaction in the latter endo TSs is achieved at the expense of peroxy acid distortion and higher steric crowding with respect to their syn,endo′ and, in particular, syn,exo counterparts.

It is worth stressing that in either syn,exo or syn,endo′ TSs both the proximal and distal peroxy oxygen seem to be involved in hydrogen bonding in a bridged hydrogen bond structure. Actually, the proximal oxygen is quite close to the hydroxylic hydrogen (OH- - -$O_7 \sim$ 2.0−2.2 Å) while the hydrogen bond to the distal oxygen (OH- - -O_8 $\sim$ 2.7−2.9 Å) takes advantage of the relatively large electronic density that resides on this center as well as of the good alignment of the three atoms involved, namely O−H- - -$O_8 \sim 163-173°$. The latter value is quite similar to the experimental datum reported by Caminati et al. for the hydrogen bond between water and the parent oxirane.[29]

As far as geometry of the cyclohexenol moiety is concerned, one can ask what changes take place on passing from ground state conformers to related hydrogen bonded TSs. The largest variation is represented by the

(29) Caminati, W.; Moreschini, P.; Rossi, I.; Favero, P. G. *J. Am. Chem. Soc* **1998**, *120*, 11144.

Table 7. Electronic Energies (hartree), Relative Electronic Energies ($E^{\ddagger}_{rel}$, kcal/mol), Electronic Activation Energies ($\Delta E^{\ddagger}$), Activation Parameters [$\Delta H^{\ddagger}$, $\Delta S^{\ddagger}$, $\Delta G^{\ddagger}$ (gas phase), and $\Delta G^{\ddagger}_{sol}$ (solution)], Relative Free Enthalpies [$G^{\ddagger}_{rel}$ (gas phase) and $G^{\ddagger}_{sol,rel}$ (solution)] for PFA Epoxidation of Cyclohexene at the B3LYP/6-311+G//B3LYP/6-31G* Level[a]**

TS	energies	$E^{\ddagger}_{rel}$	$\Delta E^{\ddagger}$	$\Delta H^{\ddagger}$	$\Delta S^{\ddagger b}$	$G^{\ddagger}_{rel}$	$\Delta G^{\ddagger}$	$\delta G^{\ddagger}_{sol}$	$G^{\ddagger}_{sol,rel}$	$\delta\Delta G^{\ddagger}_{sol}$	$\Delta G^{\ddagger}_{sol}$
cyclohexene	−234.713102							−1.31			
exo-**4**	−499.670196	0.00	9.82	10.29	−28.11	0.00	18.12	−2.03	0.00	0.15	18.27
endo-**4**	−499.667761	1.53	11.35	11.88	−28.65	1.74	19.86	−1.69	2.08	0.49	20.35

[a] See footnotes of Table 5. [b] Statistical reaction factors (i.e., accounting for the presence of two equivalent faces in cyclohexene) are included in molar activation entropies

Scheme 2

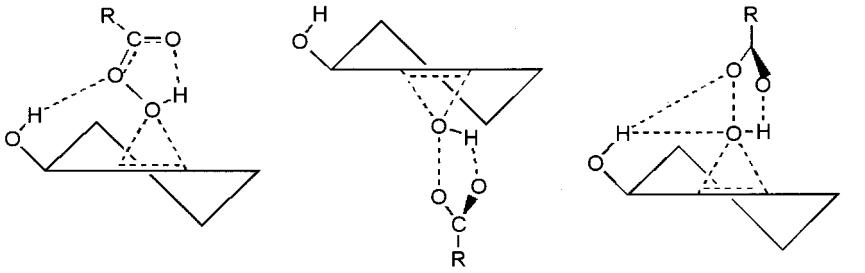

L (planar syn TS) **M** (spiro anti,exo TS) **N** (spiro syn,exo TS)

considerable adjustment of the H−O−C_1−C_2 dihedral angle for all TSs while a significant distortion of the O−C_1−C_2−C_3 dihedral angle takes place in *syn,endo′,-eq*-**5** (∼6°), *syn,endo,ax*-**5** (∼9°), and *syn,endo′,ax*-**5** (∼11°) (Table 4).

Hydrogen bonding influences asynchronicity in bond formation. In anti attacks, asynchronicity mainly reflects the need to increase staggering between one incipient C- - -O_7 bond and the syn allylic axial C−H bond [C_1−H in TSs *anti,eq*-**5** and C_4−H in TSs *anti,ax*-**5**]. In the case of syn attacks, asynchronicity is best interpreted as the result of the tendency to improve hydrogen-bonding interaction. The latter observation is particularly true in the case of the most asynchronous syn TSs (that is, *syn,exo,eq*-**5** and the two syn,endo′ TSs) in which the shorter forming bond (C_2- - - -O_7) is that one next to the OH group as a result of the shift of the O_7- - -O_8 peroxy system toward OH.

Spiro vs Planar Orientation. *Another important aspect of the peroxy acid epoxidation mechanism is the choice between a spiro and planar TS, which in principle could be driven by hydrogen bonding.* We have already stressed that in the case of epoxidation of cyclohexene derivatives one cannot expect a perfect spiro geometry, namely, with the peroxy acid plane perpendicular to the C═C bond axis. Thus, also in anti TSs (exo and endo) from both *eq*-**1** and *ax*-**1**, the γ and $H_{11}O_7XC_2$ angles deviate somewhat from 90°, but deviation never exceeds 15° (Table 4). These transition structures must be classified as spiro, and the same descriptor must be used for *syn,exo,eq*-**5** and *syn,exo,ax*-**5**.

The latter TSs resemble the qualitative model proposed by Sharpless et al. but to reconcile this proposal with calculations one must replace the γ value of 60° (see **C**, Figure 1) with ∼100° and ∼80° for epoxidation of pseudoequatorial and pseudoaxial cyclohexenols, respectively, and assume that hydrogen bonding involves both the peroxy oxygens.

Deviation from the ideal spiro structure (γ and $H_{11}O_7$-XC_2 = 90°) is quite large in syn,endo′ TSs (by ∼40° for both angles) as well as in syn,endo TSs (by 35−30° for γ) and for the latter TSs classification is compounded by the out of plane distortion of the peroxy acid moiety. However, syn,endo TSs can be safely classified as spiro-like TSs given that the $H_{11}O_7XC_2$ dihedral angle (∼ 72°) remains close to 90°. Only syn,endo′ TSs exhibit a structure that is almost halfway (γ and $H_{11}O_7XC_2$ ∼ 128−133°) between a spiro and a planar TS.

A relatively large deviation from spiro geometry can be achieved in peroxy acid epoxidation TSs, to accommodate steric interaction and strengthen hydrogen bonding, but TS geometry always remains a spiro-like geometry. Only in very particular cases (as in the case of sesquinorbornene derivatives) the reacting system seems to be forced, by very stringent geometrical restraints, to adopt a planar-like TS.[30] *One can confidently states that planar-like TSs cannot be operative in peroxy acid epoxidation of the vast majority of alkene derivatives. Thus, the "wrong" planar approach between reactants commonly used in textbooks*[31] *to illustrate the attack by peroxy acid to olefin and allylic alcohols (e.g.,* **L** *in Scheme 2)*[31a] *must be replaced by the "correct" spiro approach.*

Energetics of Cyclohexene and Cyclohexenol Epoxidation. Facial Selectivity and Reaction Rates.

Dominant Transition Structures: syn,exo vs syn,-endo TSs and syn vs anti TSs. We first address the problem of competition between syn,exo TSs with hydrogen bonding to peroxy oxygens and syn,endo TSs with hydrogen bonding to carbonyl oxygen.

In all the qualitative models, advanced by experimentalists for epoxidation of cyclic and acyclic allylic alcohols, the OH group hydrogen bonds the peroxy oxygens. In contrast, calculations for acyclic allylic alcohols clearly show that actually the two mechanisms compete with each other. However, as mentioned in Computational Methods, one disturbing feature emerges from calculation on the reaction of acyclic alcohols; that is, the observation that the relative potential energies of the two kinds of TSs depend on the theory level and can be reversed on passing from B3LYP/6-31G* to B3LYP/6-311+G** method since the latter method favor syn,exo over syn,endo TSs.[13,14]

Table 8. Comparison between the Experimental ($\Delta G^{\ddagger}_{exp}$ and k_{exp})[a] and Theoretical ($\Delta G^{\ddagger}_{sol,app}$ and k_{theor})[b] Data for Peroxy Acid Epoxidation of Cyclohexene and Cyclohexenol Derivates

	$\Delta G^{\ddagger}_{exp}$	$\Delta G^{\ddagger}_{sol,app}$[b]	$k_{exp} \times 10^3$	$k_{exp,rel}$	$k_{theor} \times 10^3$	$k_{theor,rel}$
cyclohexene	18.95	18.26	6.33	1.00	22.08	1.00
2-cyclohexen-1-ol	19.29	19.29	3.4	0.55	3.39	0.15
cis-5-*tert*-butyl-2-cyclohexen-1-ol	19.15	19.03	4.8	0.75	5.45	0.25
trans-5-*tert*-butyl-2-cyclohexen-1-ol	20.24	19.86	0.67	0.10	1.20	0.05

[a] Reference 6. [b] Calculated from B3LYP/6-311+G**//B3LYP/6-31G* potential energy. Contribution of molecular motions from B3LYP/6-31G* geometry.

What about cyclohexenols? Also in the case of cyclic derivatives there is a basis set effect on TS relative energies *but the syn,exo vs syn,endo choice is now straightforward*. In fact, the potential energy of syn,exo TSs (hydrogen bonded to peroxy oxygens) is significantly lower (by ~1.3 kcal/mol) than that of the corresponding syn,endo TSs (hydrogen bonded to carbonyl oxygen) already at the B3LYP/6-31G* level (Table S1), and this difference increases (to ~2.7−2.8 kcal/mol) on passing to the B3LYP/6-311+G**//B3LYP/6-31G* method (Table 5). Entropic effects and solvent effects (benzene) add a further favor (both of ~0.5 kcal/mol) to the former TSs with respect to the latter ones. As a result, syn,exo TSs are considerably more stable (by ~3.8 kcal/mol) than related syn,endo (and by ~3.0 than syn,endo′) TSs at the higher computational level with inclusion of solvent effects ($G^{\ddagger}_{sol,rel}$, Table 5).

Exo TSs clearly outweigh endo TSs also in the case of anti attack to cyclohexenols as a result of the higher steric crowding in the latter TSs than in the former ones. This observation also holds for the cyclohexene reaction.

*In short, the peroxy acid epoxidation of cyclic alkenes affords epoxides only via exo TSs, e.g., syn,exo,eq-**5** and syn,exo,ax-**5** for syn epoxides and anti,exo,eq-**5** and anti,-exo,ax-**5** for anti epoxides in the case of epoxidation of eq-**1** and ax-**1**, respectively.*

As for facial selectivity, hydrogen bonding stabilization of syn TSs is clearly reflected in their lower potential energy with respect to anti TSs. However the latter TSs are favored by entropic and solvent effects so that the syn−anti stability gap is highly reduced when the B3LYP/6-311+G*//B3LYP/6-31G* solution free enthalpy ($G^{\ddagger}_{sol,rel}$, Table 5) is considered and anti,exo TSs become more stable than related syn,endo as well as syn,endo′ TSs. In short, we have a syn,exo/anti,exo TS pair, for the reaction of either *eq*-**1** (*syn,exo,eq*-**5**/*anti,exo,eq*-**5**) or *ax*-**1** (*syn,exo,ax*-**5**/*anti,exo,ax*-**5**), which is considerably more stable than other competing TSs and controls facial selectivity.

It is gratifying to conclude that, in accord with our preliminary computational data on cyclobutenol epoxidation,[13] *facial selectivity in peroxy acid epoxidation of cyclic allylic alcohols can qualitatively be discussed on the basis of only two TSs, namely the anti,exo and syn,exo TS, the latter with hydrogen bond to peroxy oxygens* (e.g., **M** and **N** in Scheme 2 for cyclohexenol reaction).

Prevalence of syn attack (theoretical for compounds **1** and experimental for compounds **2**) is higher in the reactions of pseudoequatorial conformers than in those of pseudoaxial conformers. We are not able to rationalize this difference. In fact, there is not any evidence (e.g., in geometries or in OH stretching frequencies) suggesting that the pseudoequatorial OH can lead to a stronger hydrogen bond, in TSs originating from *eq*-**1**, than the pseudoaxial OH, in TSs arising from *ax*-**1** (or vice versa). Consequently, the different diastereoselectivity, observed for the two conformers, is not traceable back to differential hydrogen bonding effects and no other factors (such as differential steric congestion or geometrical distortion in syn as compared to anti TSs for the two conformers) clearly emerge as possible explanations.

Theoretical Prediction vs Experimental Data. Our higher level (B3LYP/6-311+G**//B3LYP/6-31G*) calculations predict a clear-cut dominance of syn attack (99% for gas phase and 95% for benzene solution) over anti attack for the reaction of *eq*-**1** and a slight attenuation of diastereoselectivity for the epoxidation of *ax*-**1** (96% for gas phase and 89% for benzene solution). The facial selectivity predicted for cyclohexenol epoxidation (i.e., the composite result of the competing reaction of the two conformers) is obviously intermediate: 98% for gas phase and 94% for benzene solution. These theoretical predictions conform well to the observed experimental diastereoselectivity in benzene solution [syn attack (%): 91% for 2-cyclohexen-1-ol, 84% for *trans*-5-*tert*-butyl-2-cyclohexen-1-ol (OH pseudoaxial), and 96% for *cis*-5-*tert*-butyl-2-cyclohexen-1-ol (OH pseudoequatorial) (Table 1)][3a] and, in particular, correctly reproduce the higher facial selectivity of the pseudoequatorial with respect to the pseudoaxial conformer.

Also the absolute activation free enthalpies are fairly well reproduced by B3LYP/6-311+G**//B3LYP/6-31G* calculations as shown by data of Table 8 where the experimental reaction rate constants and the related $\Delta G^{\ddagger}$ (k_{exp} and $\Delta G^{\ddagger}_{exp}$ for cyclohexene, cyclohexenol, and cis- and *trans*-5-*tert*-butylcyclohexenol) are compared to the theoretical reaction rate constants and the related "apparent" $\Delta G^{\ddagger}$ [$\Delta G^{\ddagger}_{sol,app}$ for cyclohexene, cyclohexenol, pseudoaxial and pseudoequatorial cyclohexenol, evaluated by taking into account all the possible reaction pathways]. It is noteworthy that, in accord with experimental data, pseudoequatorial cyclohexenol is predicted to be more reactive than pseudoaxial cyclohexenol, and cyclohexene more reactive than cyclohexenol.

However, the latter correct prediction is achieved only at the higher theory level with introduction of solvent effect because with the B3LYP/6-31G* method the cyclohexenol reaction in gas phase is predicted to be slightly faster than cyclohexene (Table S2). It is worth noting that activation electronic energies are enhanced on going from B3LYP/6-31G* to B3LYP/6-311+G** basis set and that this variation is larger for cyclohexenol than for cyclohexene, for syn than for anti attacks and for endo than for exo TSs. Moreover, solvent effects increase the activation free enthalpy more for cyclohexenol than for cyclohexene epoxidation (by ~1.0 kcal/mol in benzene).

A direct comparison of experimental $\Delta H^{\ddagger}$ and $\Delta S^{\ddagger}$ (solution data) and corresponding to theoretical parameters (gas-phase data) is not possible. However, on passing from the exo attack on cyclohexene ($\Delta H^{\ddagger} = 10.29$ kcal/mol) to the anti,exo attack on both pseudoequatorial

and pseudoaxial cyclohexenol ($\Delta H^{\ddagger}$ = 12.01 and 12.35 kcal/mol, respectively) and then to the syn,exo attack on both pseudoequatorial and pseudoaxial cyclohexenol ($\Delta H^{\ddagger}$ = 9.33 and 9.94 kcal/mol, respectively) we observe a trend in gas phase theoretical activation enthalpies very similar to that reported for the corresponding experimental activation parameters (benzene solution) ($\Delta H^{\ddagger}$ = 10.42, 12.36 and 8.35 kcal/mol for perbenzoic acid epoxidation of cyclohexene, 3-methoxycyclohexene and 2-cyclohexen-1-ol, respectively). That is, calculations correctly describe the increase in activation enthalpies (rate retardation) due to the electron-attracting effect of the OH (OMe) group as well as the decrease in the same parameter (rate acceleration) due to the stabilizing hydrogen bonding interaction that overcomes the inductive effect.[32]

The trend of the theoretical activation entropies ($\Delta S^{\ddagger}$ = −28.2, ∼−30.0, and ∼−31.5 eu for exo attack on cyclohexene, anti,exo and syn,exo attacks on cyclohexenol, respectively) does not corresponds to that of experimental values (−32.9, ∼−30.7, and ∼−41.0 eu, for cyclohexene, 3-methoxycyclohexene, and 2-cyclohexen-1-ol, respectively) and it is quite disturbing that the theoretical datum does not reproduce the very negative value found for cyclohexenol epoxidation. Calculations correctly suggest that formation of hydrogen bond in TSs gives rise to a more negative activation entropy (and the stronger the bond the higher this effect); however, the predicted entropy decrease is smaller than that observed experimentally. Given the limited number of data as well as the uncertainty about entropy correction to be introduced on passing from gas phase to condensed phase,[23c] it is not possible to draw definitive conclusions on this point. We are now trying to produce further experimental activation entropy data to clarify this problem.

Conclusions

B3LYP calculations demonstrate that several reaction pathways can, in principle, compete each other in producing the final epoxides in the peroxy acid epoxidation of both the pseudoequatorial and pseudoaxial cyclohexenol conformers. However, these computational data provide convincing evidence that the actual competition (which determines epoxidation facial selectivity) takes place between only two TSs, that is, a syn,exo and an anti,exo TS for both conformers. The syn,exo TSs are more stable than their anti,exo competitors because they benefit from an attractive hydrogen bond interaction (involving both the peroxy oxygens) that overrides the unfavorable entropic and solvation effects. Qualitative predictions and rationalizations of facial selectivity in cyclic alcohols epoxidations by peroxy acids must be based on these TSs.

It is also worth stressing that (i) all TSs located for the reactions under study exhibit a spiro-like structure [namely, with the dihedral angle between the peroxy acid plane and the forming oxirane plane closer to 90° than to 0° (or 180°)], (ii) syn,endo TSs with hydrogen bonding to carbonyl oxygen are definitely less stable than the corresponding syn,exo TSs in which the olefinic OH group hydrogen bonds the two peroxy oxygens.

The facial selectivity theoretically predicted for pseudoequatorial and pseudoaxial cyclohexenol nicely conforms to the experimental stereoselectivity reported for cyclohexenol and *cis*- and *trans*-5-*tert*-butyl-2-cyclohexen-1-ol (with OH in pseudoequatorial and pseudoaxial position, respectively). In fact, dominance of syn-OH attack for both conformers as well as the higher syn-selectivity observed for the epoxidation of the pseudoequatorial as compared to that of the pseudoaxial isomer is very well reproduced.

Also absolute and relative theoretical reaction rate constants compare fairly well with experimental data. Interestingly, calculations confirm the suggestion[3a] that the slight higher reaction rate constant of cyclohexene as compared to cyclohexenol epoxidation is the result of entropic and solvation effects that favor TSs of the former reaction and overcome the stabilizing hydrogen bonding effect present in syn TSs of the latter reaction.

Acknowledgment. Financial support from MURST and CNR is gratefully acknowledged.

Supporting Information Available: Electronic energies, molecular motion contributions and activation parameters (gas phase and solution) for PFA epoxidation of 2-cyclohexen-1-ol and cyclohexene at the B3LYP/6-31G* level reported. This material is available free of charge via the Internet at http://pubs.acs.org.

JO000900Y

(30) Koerner, T.; Slebocka-Tilk, H.; Brown, R. S. *J. Org. Chem*. **1999**, *64*, 196. However, computational work, actually in progress in our laboratory, has already demonstrated that a "forced" planar-like TS shows a very high incipient bond asynchronicity, namely, it lies in the borderline region between concerted and nonconcerted processes.

(31) (a) Robinson, M. J. T. *Organic Stereochemistry*; Oxford Science Publications: New York, 2000; p 78. (b) Procter, G. *Stereoselectivity in Organic Synthesis*; Oxford Science Publications: New York, 1998; p 18.

(32) For previous discussions, based on computational data, on the alkene/allylic alcohol competition in epoxidation reaction with peroxy-acids, see ref 12, and with dioxiranes, see Freccero, M.; Gandolfi, R.; Sarzi-Amadè M.; Rastelli, A. *Tetrahedron* **1998**, *54*, 12323. These papers also conclude that the lower rectivity of allylic alcohols vs the corresponding alkene cannot be traced back only to inductive effects.